*Proceedings of the 35th European Safety and Reliability & the 33rd Society for Risk Analysis Europe Conference*
*Edited by* Eirik Bjorheim Abrahamsen, Terje Aven, Frederic Bouder, Roger Flage, Marja Ylönen

doi: 10.3850/978-981-94-3281-3_ESREL-SRA-E2025-P9012-cd

# Simulation and Risk Assessment of $CO_2$ Buried Pipeline Leakage and Diffusion Using PHAST

Yan Shang[1], Ming Yang[1], Xiaoling Chen[2], Xiaokai Xing[1,2,3], Guoyu An[1], Jian Jiao[1], Jianzhang Zhao[2], and Mengjie Yu[1]

[1]*College of Mechanical and Transportation Engineering, China University of Petroleum, Beijing, China.*

*shangyan_cup@163.com, ym13160061139@163.com, xingxiaokai@vip.sina.com, 1258419196@qq.com, jiaojian_cup@163.com, 1571431943@qq.com*

[2]*Engineering Institute, China University of Petroleum, Karamay, China.*

*cxling612@cupk.edu.cn, 2023216911@st.cupk.edu.cn*

*3 Autonomous Region Tianshan Innovation Team for Research and Application of High-Efficiency Oil and Gas Pipeline Technology, Xinjiang, China.*

Carbon dioxide pipeline leaks can pose significant threats to human health and environmental safety. This study utilized PHAST software to simulate far-field $CO_2$ dispersion, validated against experimental results. Key factors analysed include leakage characteristics (direction and size), pipeline parameters (operating pressure and fluid temperature), and environmental conditions (wind speed, atmospheric stability, and ambient temperature), with thresholds of 0.5% and 5.0% $CO_2$ volume as safety and lethal limits, respectively. Results show middle perforations cause wider horizontal dispersion near the ground, while high-consequence areas (HCAs) expand with increasing operating pressure, leak size, and ambient temperature, but decrease with higher wind speed and atmospheric stability. Leakage size was identified as the most critical factor, with HCAs growing exponentially with size. This study provides a scientific basis for $CO_2$ leakage risk assessment and offers guidance to enhance pipeline safety in CCUS systems.

*Keywords*: $CO_2$ buried pipeline; small hole leakage; diffusion concentration; high-consequence areas (HCAs) PHAST.

## 1. Introduction

As a critical link in the CCUS technology chain, $CO_2$ pipeline transportation plays a fundamental role in enabling large-scale deployment of CCUS infrastructure. (Balaji and Rabiei, 2022; Hill et al., 2020) Unlike conventional oil and gas pipelines, $CO_2$ pipelines typically operate under supercritical or dense-phase conditions, which demand higher pressures and pose unique safety challenges. Ensuring the safe operation of these pipelines is therefore paramount. (X. Wang et al., 2023) However, pipelines are subject to significant risks of leakage, primarily due to mechanical damage, corrosion, third-party interference, and natural disasters. (Zhang et al., 2022) Although $CO_2$ is neither toxic nor flammable, it is highly asphyxiating. Its density, which exceeds that of air, causes leaked $CO_2$ to accumulate near the ground, forming high-concentration zones that can lead to suffocation, injuries, or fatalities for humans and animals in the vicinity. Additionally, $CO_2$ leakage can exacerbate the greenhouse effect. (P. Wang et al., 2023)

Over the past decade, extensive research on $CO_2$ pipeline leakage has been conducted at both national and international levels. (Yan et al., 2018; Gu et al., 2019; Wang et al., 2021) Most studies primarily focus on above-ground pipelines, while research on buried pipeline leakage remains relatively limited. (Shang et al., 2024) Leakage incidents can be classified based on the size of the leak: small hole (where the ratio of the leak size to the pipeline diameter is $d/D < 0.2$), large hole ($0.2 \leq d/D < 0.6$), and full pipeline ruptures ($d/D \geq 0.6$). (Meribout et al., 2020) Among these types, small hole leakage is particularly concerning due to its multiple leakage points, strong concealment, difficulty in detection, and high potential danger. (Ding et al., 2023) Munkejord et al. (2020) constructed a $CO_2$ leakage experimental platform with medium recycling capability, revealing that the depressurization rate is faster in the dense phase than in the supercritical phase. This difference was attributed to the lower initial temperature and higher compressibility of dense-phase $CO_2$. Guo et al. (2016, 2017) investigated the near-field leakage behavior of overhead pipelines by analyzing the position of Mach disks and the morphology of visible clouds. Their results showed that larger leakage hole sizes or higher leakage volumes significantly increase the low-temperature jet region and the $CO_2$ diffusion radius. Similarly, Teng et al. (2018) conducted small-hole $CO_2$ leakage experiments using high-pressure gas cylinders and nozzles. They measured a maximum fluid velocity of 250 m/s near the leakage point and observed that $CO_2$ concentrations along the leakage axis initially rise and then decline. In terms of far-field dispersion, the primary concern of $CO_2$ pipeline leakage lies in the concentration distribution, which fundamentally differs from the heat radiation mechanism observed in natural gas pipeline leaks. The diffusion process is influenced by leakage volume, atmospheric stability, and environmental conditions. Hu et al. (2022) demonstrated that as the leakage hole size increases, jet intensity and visible cloud dissipation rates also rise. Furthermore, they identified a hazardous zone extending up to 80 meters laterally from the leakage axis and 8 meters longitudinally.

Two main methodologies are commonly employed for $CO_2$ leakage and dispersion simulations: CFD-based simulation software and engineering simulation software. Computational fluid dynamics (CFD) tools, such as FLUENT, OpenFOAM, and COMSOL, offer detailed and precise modeling but are computationally intensive. In contrast, engineering simulation tools, such as PHAST, SAFETI, and ALOHA, are computationally efficient and capable of delivering results in a shorter timeframe. (Shang et al., 2024) Among these, PHAST (Process Hazard Analysis Software Tool) is widely used in industrial applications, including petroleum, natural gas, and chemical industries, to simulate the leakage and dispersion of hazardous substances. (You and Kim, 2020; James and Renjith, 2021) Wang et al. (2021) utilized PHAST software to simulate the hydrogen diffusion distance, explosion, and jet fire radiation safety distances at a hydrogen refueling station under specific conditions, while also supplementing existing standards. Zhong et al. (2024) employed PHAST to simulate various tank leakage scenarios and developed a tank incident database that enabled effective prediction of the impact range of fire events in tank areas. Witlox et al. (2018) conducted verification and validation of the PHAST consequence models based on extensive experimental data for accidental releases of toxic or flammable chemicals into the atmosphere. The simulation results have been adopted as benchmarks in the development of numerous domestic and international standards. (Pouyakian et al., 2023)

In this study, PHAST software was employed to systematically analyze the key factors influencing $CO_2$ leakage and dispersion in long-distance pipelines. The analysis clarified the effects of various parameters on the dispersion range, offering critical insights for defining hazardous zones around $CO_2$ pipelines. These findings are of significant importance for ensuring the safe operation of CCUS projects.

## 2. Model and Validation

This study employs the Unified Dispersion Model (UDM) to simulate the diffusion process of continuous $CO_2$ leakage. The UDM combines the strengths of the Gaussian, BM, and PG models, allowing for the consideration of phase change effects during $CO_2$ leakage and dispersion. The model was further refined using experimental data from the Kit Fox and BPDF1 $CO_2$ leakage experiments to enhance accuracy and reliability. (Pouyakian et al., 2023) This refined model effectively describes cloud width and downwind dispersion distances under specific meteorological conditions, capturing realistic diffusion behavior under multi-factor coupling. The concentration distribution in the diffusion model is given as (Witlox et al., 2023):

$$c(x, y, \zeta) = C_o(x) F_h(y) F_v(\zeta) \tag{1}$$

$$F_v(\zeta) = \exp\left\{ -\left| \frac{\zeta}{R_z(x)} \right|^{n(x)} \right\} \tag{2}$$

$$F_h(x,y) = \exp\left\{ -\left[ \left( \frac{x - x_{cld}(t)}{R_x(t)} \right)^2 + \left( \frac{y}{R_y(t)} \right)^2 \right]^{m/2} \right\} \tag{3}$$

$$\zeta = z - z_{cld} \tag{4}$$

Where $c$ represents the concentration profile (kg/m$^3$), expressed as a function of Cartesian coordinates $x$ (downwind distance), $y$ (cross- wind distance) and $z$ (vertical height above the ground). $F_v$ represents the vertical concentration profile of the cloud, which is defined in terms of the distance $\zeta$ (perpendicular to the plume centerline) and the vertical radius $R_z$. $F_h$ represents the horizontal concentration profile of the cloud, defined in terms of the distances $x$ and $y$ from the cloud's centerline. $R_x$ and $R_y$ represent the horizontal radius of the plume in the $x$ and $y$ directions, respectively. $m$ and $n$ denote the concentration profile exponents. $x_{cld}$ and $z_{cld}$ denote the cloud centerline position and elevation height, respectively.

To validate the accuracy of PHAST software's dispersion simulations, a $CO_2$ pipeline leakage experiment conducted by Zhu et al. (2022) was selected as a verification case. The experiment involved a 257-meter-long main pipeline with an inner diameter of 233 mm and a maximum operating pressure of 12 MPa. Conducted under windless conditions at an ambient temperature of 28°C, the setup included concentration and temperature sensors arranged on a plane at the same height as the pipeline. Additional experimental parameters are detailed in Table 1.

Table 1. Experimental parameters

| No. | Pressure (MPa) | Temperature (°C) | Leakage size (mm) | Distance of measurement points (m) |
|---|---|---|---|---|
| 1 | 7.6 | 35.1 | 15 | 5. 9, 11, 14, 17 |
| 2 | 9.0 | 35.6 | 50 | 5, 7, 9, 11, 17, 50 |

A comparison between the simulation results and experimental data (Figure 1) shows that the error in PHAST simulation results is consistently below 20%, within the acceptable range for engineering applications. This underscores the high reliability of PHAST software, confirming its effectiveness as a dependable tool for engineering design and safety evaluations.

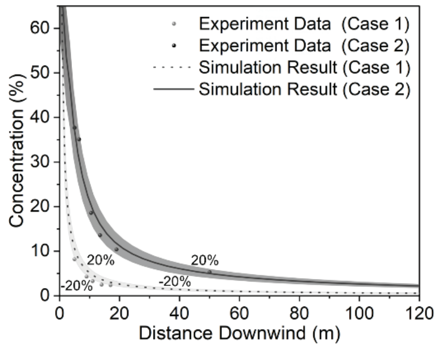


Fig. 1. Experimental verification of the numerical model.

## 3. Simulation Parameters

### 3.1 *Hazard boundaries of $CO_2$*

To quantitatively assess the toxicity of $CO_2$, the UK's Health and Safety Executive (HSE) conducted a Dangerous Toxic Load (DTL) evaluation, identifying a concentration of 50,000 ppm as the Significant Lethal Toxicity (SLOT) level. (*Occupational exposure limits for hazardous agents in the workplace*, 2019) Additionally, $CO_2$ has been incorporated into occupational safety management guidelines by the Environmental Safety Association. According to the GBZ 2.1-2019 "Occupational Exposure Limits for Hazardous Agents in the Workplace," the time-weighted average permissible concentration of $CO_2$ is 9,000 mg/m³, equivalent to 5,000 ppm (0.5%), which is considered safe for most individuals under workplace exposure conditions. (*Occupational exposure limits for hazardous agents in the workplace*, 2019) In summary, this study identifies two critical thresholds for $CO_2$ pipeline leakage risk assessment: 5,000 ppm (0.5%) as the occupational safety limit and 50,000 ppm (5.0%) as the lethal hazard concentration. (*Assessment of the Dangerous Toxic Load (DTL) for Specified Level of Toxicity (SLOT) and Significant Likelihood of Death (SLOD)*.)

### 3.2 *Model construction*

This study examines a proposed long-distance $CO_2$ pipeline project as the research background. The pipeline is designed to operate at a pressure of 12

MPa, with dimensions of D273×11.1 mm, and is buried at a depth of 1.5 m. Constructed from L415M high-frequency resistance-welded steel, the pipeline has a wall roughness of 0.045 mm and a total length of 44.7 km. The system includes a starting station, an end station, and an intermediate valve room located 21.8 km from the starting station. The entire route has flat terrain.

Using the pipeline segment between the starting station and the intermediate valve room as a case study, this research analysed the influence of leakage characteristics (leakage direction and size), pipeline properties (operating pressure and temperature), and environmental conditions (wind speed, atmospheric stability, and ambient temperature) on the extent of high-consequence areas. The simulation conditions are summarized in Table 2.

Table 2. Basic parameters of work scenarios.

| Leakage direction | Top, middle, bottom |
|---|---|
| Leakage size (mm) | 1, 3, 5, 10, 20, 30, 40, 50 |
| Operating Pressure (MPa) | 10, 12 |
| Fluid Temperature (°C) | 20, 40 |
| Wind Speed | 1.5, 3, 5, 7, 10, 12 |
| Atmospheric Stability | B, D, F |
| Ambient Temperature (°C) | -10, 10 |

## 4. Results and Discussion

### 4.1 *Leakage characteristics*

#### 4.1.1 *Leakage direction*

This study analyses the impact of leakage direction on the HCAs of $CO_2$ diffusion from pipelines. The distribution of $CO_2$ concentrations at 0.5% under three leakage directions is illustrated in Figure 2, revealing significant differences in diffusion behaviour between buried and overhead pipelines.

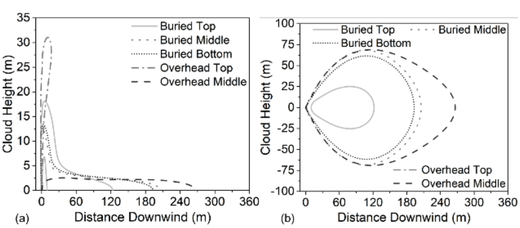


Fig. 2. Diffusion range of $CO_2$ at different leakage direction (top, middle and bottom). (a) Side view (b) Maximum diffusion range.

For buried pipelines, leakage gas is influenced by soil resistance, regardless of whether the leakage occurs at the top, middle, or bottom of the pipe. $CO_2$ must penetrate the soil to reach the surface, and after emerging, it retains a certain level of kinetic energy, causing its initial diffusion to be directed vertically upward. As the kinetic energy dissipates, gravitational forces dominate, leading to gas accumulation in the near-ground layer and the formation of a potential high-risk area. In contrast, overhead pipelines exhibit free-jet diffusion behaviour. When leakage occurs at the top of the pipeline, the gas primarily diffuses vertically upward, with no significant $CO_2$ accumulation near the ground due to the high jet velocity (Figure 2b). In cases where leakage occurs at the middle of the pipeline, $CO_2$ diffuses horizontally, forming larger HCAs at ground level. Compared to perforations at the top or bottom of buried pipelines, middle perforations result in a broader horizontal diffusion range of $CO_2$ near the ground surface. This occurs because middle perforations allow $CO_2$ to diffuse horizontally within the soil over a longer path before reaching the surface, releasing gas simultaneously from multiple diffusion points. To ensure the safety of personnel near the pipeline, subsequent analyses in this study focus on middle perforation scenarios.

#### 4.1.2 *Leakage size*

This section examines the effect of varying small-hole leakage sizes on the hazardous diffusion range of $CO_2$. As shown in Figure 3, increasing the leakage hole diameter from 3 mm to 10 mm expands the horizontal diffusion range of $CO_2$ at a concentration of 0.5% from 31.8 m to 205.4 m, while the vertical diffusion height increases from 6.5 m to 12.3 m. The diffusion area also grows significantly, from 307 m² to 20,111 m². For a CO2 concentration of 5.0%, the vertical cloud height rises from 3.7 m to 9.6 m.

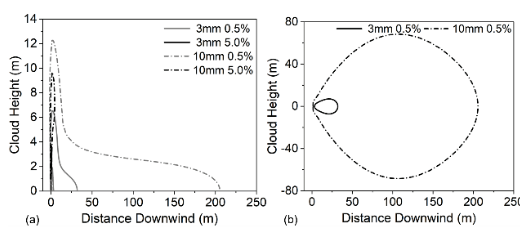

Fig. 3. Diffusion range of $CO_2$ at different leakage size (3mm, 10mm). (a) Side view (b) Maximum diffusion range.

The results reveal that as leakage hole size increases, the horizontal diffusion distance and area of $CO_2$ near the ground follow an approximately logarithmic growth trend (Figure 4). This behaviour is attributed to larger leakage holes releasing greater volumes of gas, imparting higher initial momentum and faster diffusion velocities to the $CO_2$. However, due to pipeline capacity limitations, the growth rate of the diffusion distance and area gradually slows down once the leakage hole diameter exceeds a certain threshold. Therefore, prompt and effective measures are essential to prevent the expansion of small-hole leakages, such as those caused by pitting corrosion, to mitigate severe safety risks and potential environmental damage.

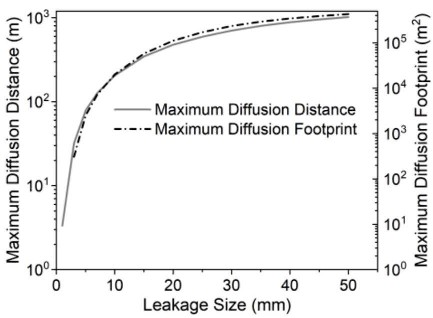


Fig. 4. Horizontal dispersion distance and range corresponding to different (small) leakage sizes.

## 4.2 *Fluid parameters*

### 4.2.1 *Operating pressure*

This section evaluates the effect of operating pressure on the extent of the HCAs during $CO_2$ leakage. As shown in Figure 5a, at a pressure of 10 MPa, the maximum diffusion height for a 0.5% $CO_2$ concentration reaches 11.3 m, with the farthest diffusion distance extending to 194.7 m. When the pressure increases to 12 MPa, the maximum diffusion height rises to 12.3 m, and the farthest diffusion distance expands to 205.4 m. Figure 5b shows the maximum diffusion footprint of the 0.5% $CO_2$ cloud. At 10 MPa, the footprint is 18,095 m², while at 12 MPa, it increases to 20,111 m².

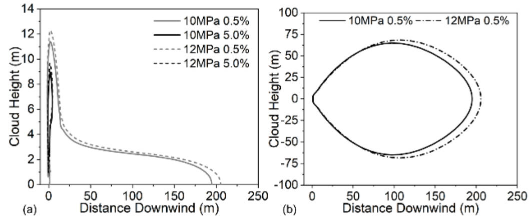


Fig. 5. Diffusion range of $CO_2$ at different operating pressures (10 MPa, 12 MPa). (a) Side view (b) Maximum diffusion range.

In summary, higher pipeline pressures result in a larger diffusion range of $CO_2$, thereby expanding the HCAs. Accordingly, when defining pipeline hazardous zones, calculations should be based on the maximum design pressure of the pipeline.

### 4.2.2 *Fluid temperature*

This section analyses the impact of fluid temperature on the extent of the HCAs during $CO_2$ leakage under the design operating pressure conditions. The findings indicate that fluid temperature significantly influences the diffusion range of the HCAs. As temperature increases, $CO_2$ density decreases, resulting in a notable rise in vertical diffusion height. For instance, at 40°C, the maximum diffusion height for 0.5% $CO_2$ concentration reaches 19.1 m, compared to 12.3 m at 20°C. Conversely, as temperature decreases, the increased density of $CO_2$ promotes horizontal diffusion near the ground surface, substantially expanding the horizontal diffusion range. At 20°C, the horizontal diffusion distance for 0.5% $CO_2$ concentration extends to 205.4 m, compared to 171.1 m at 40°C. Similarly, the maximum diffusion footprint of 0.5% $CO_2$ concentration near the ground increases from 92,112 m² at 40°C to 201,111 m² at 20°C.

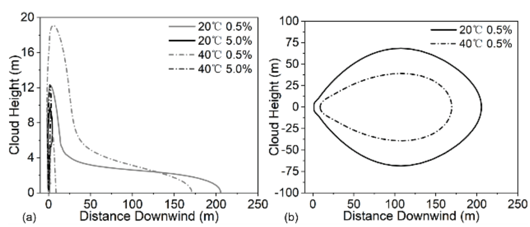


Fig. 6. Diffusion range of $CO_2$ at different fluid temperatures (20°C, 40°C). (a) Side view (b) Maximum diffusion range.

In conclusion, $CO_2$ leakage under low-temperature conditions results in a broader horizontal diffusion range and greater accumulation near the ground surface, leading to an expanded hazardous area and increased risks to the surrounding environment and personnel safety. To mitigate these risks, hazardous zone calculations should be based on the minimum allowable inlet temperature.

### 4.3 *Environment conditions*

### 4.3.2 *Wind speed and atmospheric stability*

This section examines the impact of wind speed and atmospheric stability on the extent of the HCAs, as shown in Figure 7. The results indicate that wind speed significantly affects the diffusion intensity and concentration distribution of $CO_2$. Higher wind speeds enhance diffusion intensity, allowing $CO_2$ to be more effectively diluted and dispersed, thereby reducing the size of high-concentration areas. This effect is particularly pronounced under low wind speed conditions.

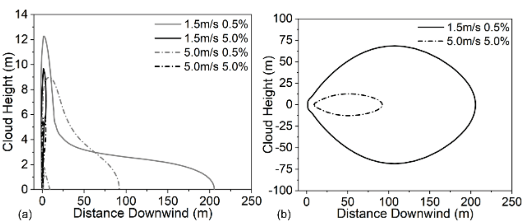


Fig. 7. Diffusion range of $CO_2$ at different wind speed (1.5m/s, 5.0m/s). (a) Side view (b) Maximum diffusion range.

Additionally, the impact of different Pasquill stability categories—representing unstable (B), moderately stable (D), and stable (F) atmospheric conditions—on $CO_2$ diffusion is primarily observed in the horizontal direction (see Figure 8). The results indicate that increased atmospheric stability hinders $CO_2$ dispersion, causing the gas to accumulate more readily near the ground surface. This accumulation effect significantly enlarges the coverage of HCAs.

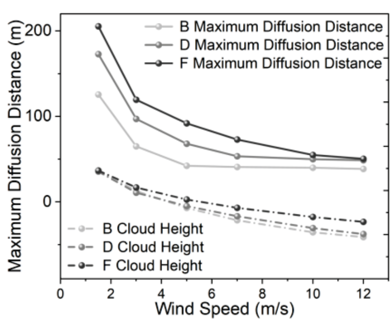


Fig. 8. $CO_2$ dispersion distance under different combinations of wind speed and atmospheric stability.

Therefore, to ensure the safety of individuals near the pipeline, it is recommended to use a wind speed of 1.5 m/s and F-level atmospheric stability as the basis for hazardous zone calculations in risk assessments. This approach provides a comprehensive evaluation under the most unfavourable conditions.

### 4.3.2 *Ambient temperature*

Under conditions of a wind speed of 1.5 m/s and F-level atmospheric stability, this section examines the impact of ambient temperature on the extent of the $CO_2$ leakage HCAs. As shown in Figure 9, increasing the ambient temperature from -10℃ to 10℃ causes the horizontal diffusion distance for a 0.5% $CO_2$ concentration to expand from 123.8 meters to 205.4 meters, while the diffusion area grows from 8,327 m² to 20,111 m². As temperature rises, the density of $CO_2$ decreases, increasing its buoyant velocity and diffusion capacity, which substantially enlarges the high-consequence zone. Under low-temperature conditions, $CO_2$ is more likely to condense or form frost, restricting its diffusion range and reducing the affected area. Conversely, at higher temperatures, $CO_2$ remains in a gaseous state, and enhanced atmospheric convection further promotes gas diffusion, expanding the coverage of the HCAs.

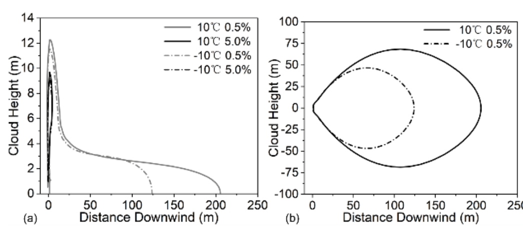

Fig. 9. Diffusion range of $CO_2$ at different ambient temperatures (-10°C, 10°C). (a) Side view (b) Maximum diffusion range.

Therefore, in summer or regions with hot climates, strengthened risk prevention and control measures should be implemented to safeguard surrounding areas.

## 5. Conclusions

This study, based on a proposed $CO_2$ pipeline project, utilized PHAST software to analyse the extent of HCAs under various operating conditions. The key findings are as follows:

- Diffusion behaviour varies significantly between buried and aboveground pipelines. For buried pipelines, middle perforations result in a greater horizontal diffusion range compared to perforations at the top or bottom, posing increased threats to the surrounding environment and personnel.
- The size of the HCAs is positively correlated with operating pressure and negatively correlated with fluid temperature. Under high-pressure and low-temperature (dense-phase) conditions, the hazard zone is at its largest. Therefore, the design pressure and minimum allowable inlet temperature should be considered critical parameters for determining the HCAs.
- Higher atmospheric stability (e.g., low wind speeds and F-level conditions) promotes $CO_2$ accumulation near the ground surface, while elevated ambient temperatures further expand the hazardous zone. Under high-temperature, low-wind, and cloudless conditions, the $CO_2$ hazard zone increases significantly.
- Leakage size was identified as the most critical factor, with HCAs growing exponentially with size. Mitigation of risks from large-aperture leaks should be prioritized. Key measures include enhancing pipeline weld strength and optimizing material selection to reduce perforation risk.

Although the PHAST software accounts for buried pipeline leakage, there remains some uncertainty in predicting crater dimensions. For instance, under initial conditions of 8 MPa and 20°C, the crater width formed by a 1 mm leak hole is 2.6 meters, which deviates significantly from experimental results. To enhance the accuracy of the model, it is recommended that PHAST further strengthen its simulation and analysis of the seepage diffusion process in the soil medium. These improvements will provide a more reliable scientific basis for buried pipeline leakage risk assessment and emergency response decision-making.

**Acknowledgement**

This work was supported by Xinjiang Uygur Region "One Case, One Policy" Strategic Talent Introduction Project (Grant No. XQZX20240054).

## References

Assessment of the Dangerous Toxic Load (DTL) for Specified Level of Toxicity (SLOT) and Significant Likelihood of Death (SLOD), HSE.

Balaji, K., Rabiei, M., 2022. Carbon dioxide pipeline route optimization for carbon capture, utilization, and storage: A case study for North-Central USA. Sustain. Energy Technol. Assess. 51, 101900.

Ding, Y., Xu, P., Lu, Y., Yang, M., Zhang, J., Liu, K., 2023. Research on Pipeline Leakage Calculation and Correction Method Based on Numerical Calculation Method. Energies 16, 7255.

Gu, S., Li, Y., Teng, L., Wang, C., Hu, Q., Zhang, D., Ye, X., Wang, J., Iglauer, S., 2019. An experimental study on the flow characteristics during the leakage of high pressure $CO_2$ pipelines. Process Safety and Environmental Protection 125, 92–101.

Guo, X., Yan, X., Yu, J., Zhang, Y., Chen, S., Mahgerefteh, H., Martynov, S., Collard, A., Proust, C., 2016. Under-expanded jets and dispersion in supercritical $CO_2$ releases from a large-scale pipeline. Applied Energy 183, 1279–1291.

Guo, X., Yan, X., Zheng, Y., Yu, J., Zhang, Y., Chen, S., Chen, L., Mahgerefteh, H., Martynov, S., Collard, A., Brown, S., 2017. Under-expanded jets and dispersion in high pressure $CO_2$ releases from an industrial scale pipeline. Energy 119, 53–66.

Hill, L.B., Li, X., Wei, N., 2020. $CO_2$-EOR in China: A comparative review. Int. J. Greenh. Gas Control 103, 103173.

Hu, Y., Yan, X., Chen, L., Yu, S., Liu, C., Yu, J., 2022. Leakage hazard distance of supercritical $CO_2$ pipelines through experimental and numerical studies. International Journal of Greenhouse Gas Control 119, 103730.

James, S., Renjith, V.R., 2021. Risk Assessment and Vulnerability Analysis of Liquefied Natural Gas (LNG) Regasification Terminal. Process Integr Optim Sustain 5, 99–121.

Meribout, M., Khezzar, L., Azzi, A., Ghendour, N., 2020. Leak detection systems in oil and gas fields: Present trends and future prospects. Flow Measurement and Instrumentation 75, 101772.

Munkejord, S.T., Austegard, A., Deng, H., Hammer, M., Stang, H.G.J., Løvseth, S.W., 2020. Depressurization of $CO_2$ in a pipe: High-resolution pressure and temperature data and comparison with model predictions. Energy 211, 118560.

Occupational exposure limits for hazardous agents in the workplace (Current No. GBZ 2.1-2019), 2019. Part 1: Chemical hazardous agents. Beijing.

Pouyakian, M., Ashouri, M., Eidani, S., Madvari, R.F., Laal, F., 2023. A systematic review of consequence modeling studies of the process accidents in Iran from 2006 to 2022. Heliyon 9, e13550.

Shang, Y., Chen, X., Yang, M., Xing, X., Jiao, J., An, G., Li, X., Xiong, X., 2024. Comprehensive Review on Leakage Characteristics and Diffusion Laws of Carbon Dioxide Pipelines. Energy & Fuels.

Teng, L., Li, Y., Hu, Q., Zhang, D., Ye, X., Gu, S., Wang, C., 2018. Experimental study of near-field structure and thermo-hydraulics of supercritical $CO_2$ releases. Energy 157, 806–814.

Wang, H., You, Z., Mo, F., Liu, B., Han, P., 2021. Study on Dispersion of Carbon Dioxide over the Shrubbery Region. Frontiers in Energy Research 9.

Wang, P., Yang, Y., Xue, D., Ren, L., Tang, J., Leung, L.R., Liao, H., 2023. Aerosols overtake greenhouse gases causing a warmer climate and more weather extremes toward carbon neutrality. Nat Commun 14, 7257.

Wang, X., Liu, Y., Liu, L., Wei, Z., Duan, R., Wang, H., Ren, X., 2023. Numerical analysis on liquid seepage - Diffusion coupled with heat in soil of low - Pressure buried pipelines leakage. Journal of Cleaner Production 406, 137157.

Witlox, Webber, Harper, D.Vstier, 2023. UDM MODEL FOR PRESSURISED INSTANTANEOUS RELEASES. DNV AS.

Yan, X., Guo, X., Yu, J., Chen, S., Zhang, Y., Mahgerefteh, H., Martynov, S., Brown, S., 2018. Flow characteristics and dispersion during the vertical anthropogenic venting of supercritical $CO_2$ from an industrial scale pipeline. Energy Procedia, Applied Energy Symposium and Forum, Carbon Capture, Utilization and Storage, CCUS 2018, 27–29 June 2018, Perth, Australia 154, 66–72.

You, C., Kim, J., 2020. Quantitative risk assessment of an amine-based $CO_2$ capture process. Korean J. Chem. Eng. 37, 1649–1659.

Zhang, J., Lian, Z., Zhou, Z., Song, Z., Liu, M., Yang, K., 2022. Leakage detection in a buried gas pipeline based on distributed optical fiber time-domain acoustic wave signal. Engineering Failure Analysis 141, 106594.

Zhong, W., Wang, S., Wu, T., Gao, X., Liang, T., 2024. Optimized Machine Learning Model for Fire Consequence Prediction. Fire 7, 114.

Zhu, G. cheng, Cao, Q., Wang, M., Yu, J. liang, Yan, X., Yu, S., Liu, C., 2022. Risk analysis of supercritical $CO_2$ release and diffusion. Journal of Safety and Environment 22, 1486–1494.